Diabetic Complications Consortium

Application Title: Validate tissue oxygenation biomarker in diabetic foot ulcers to assess healing using a low-cost hand-held optical imager

Principal Investigator: Anuradha Godavarty, Florida International University
Collaborating-PI: Dr. Robert Kirsner (University of Miami).

1. Project Accomplishments:

- Developed a near-infrared optical scanner that is capable of both static and dynamic imaging, such that it can acquire spatio-temporal maps of tissues without contact.
- Validation Studies: (a) Preliminary validation studies on phantoms gave >85% correlation in measurements compared to the standard spectrophotometer. (b) Dynamic imaging-based phantom studies gave >90% correlation in the measured oxygen saturation compared to that obtained from a standard dissolved oxygen meter. (c) In-vivo validation studies on controls validated NIROS' ability to observe temporal changes in oxygen saturation with ~90% correlation compared to a commercial device.
- This research was part of an MS student's final project in Spring 2019. Therefore, all the major aims that were accomplished are part of a doctoral student's dissertation.
- Publications/Presentations: Work was presented as posters/oral talks at four national/international level conferences (SPIE Photonics West, OSA Biomedical Congress, Innovations in Wound Healing, and BMES Annual Meeting), conference proceedings, and also internally at multiple university level conferences.
- Grants Awarded: The preliminary results from this DiaComp Pilot Grant led to an NIH F31 Pre-Doctoral Fellowship from NIDDK in 2020.

2. Specific Aims:

AIM 1: Calibration and validation of TO-based biomarker from tissue phantom studies using NIROS.

(i) Phantom validation studies (without scatterers) using Near-Infrared Optical Scanner (NIROS): Phantom studies on time-varying hemoglobin concentration changes are currently performed using our custom-developed hand-held NIROS against a commercial spectrophotometer (see Fig. 1). Methemoglobin (MHb) solutions were reduced to HbR using sodium hydrosulfite, which converted to

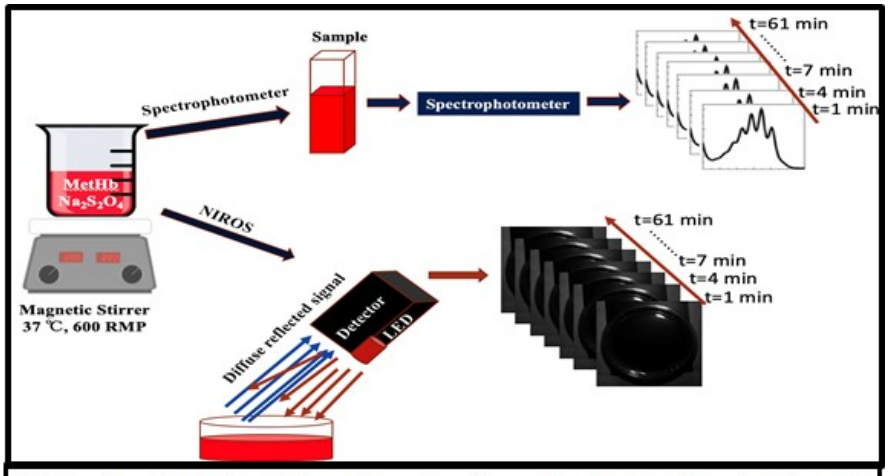

Fig. 1. Experimental set up for simultaneously implement spectrophotometer and NIROS

HbO with time. From systematic phantom studies, the changes in oxygen saturation (ΔStO_2) with time were recorded using both the devices and >85% correlation was observed across the devices (see Figs. 2, 3). These studies were carried out in non-scattering medium. The study with inclusion of scatterers into the phantom medium is described in the next sub-aim.

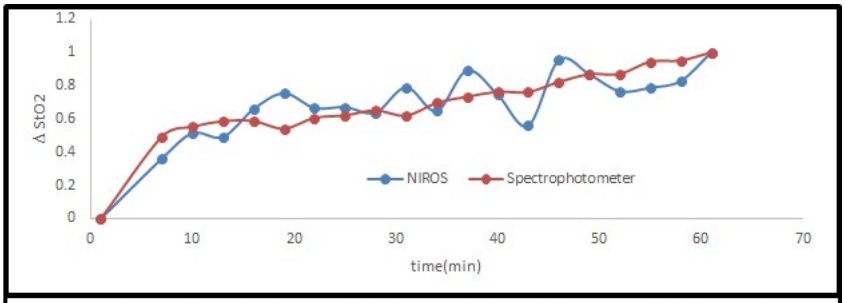

Fig 2. Change of oxygen saturation(ΔStO_2) of phantom with time using spectrophotometer and NIROS

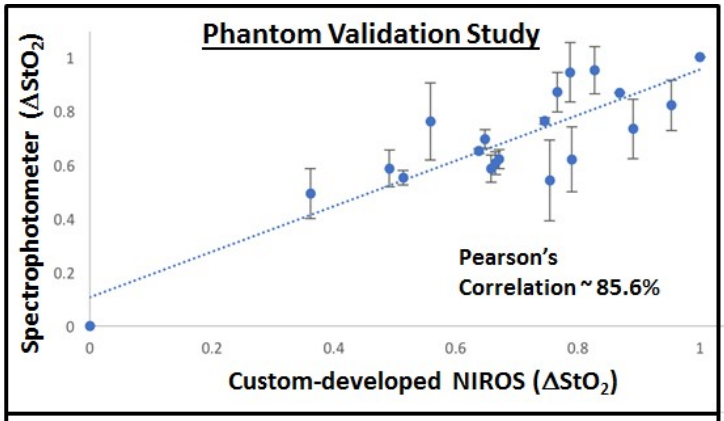

Fig. 3. Pearson's correlation of changes in oxygen saturation (ΔStO_2) from bovine hemoglobin based phantom studies using our custom NIR optical scanner (NIROS) and commercial spectrophotometer.

(ii) Phantom validation studies (with scattering agents) using NIROS:

A scattering agent was introduced into the phantom medium (using diluted milk or Intralipid solutions). Next, imaging was performed using NIROS, a thermometer, pH meter, and Dissolved Oxygen meter. Simultaneously during imaging, temperature, acidity, and dissolved oxygen (ppm) were recorded throughout the reaction. It was found that there were no significant changes in pH throughout the reaction- which can affect the amount of oxygen in the solution.

Study 1: The first study was focused on determining the background signal prior to introducing the reaction as described in the prior study. The phantom consisted of a hollow cylindrical tube (mimicking a blood vessel) subjected in a milk-based scattering solution. In this study, the vessel was filled with: Case (1) Deionized (D.I) water, and Case (2) Methemoglobin. Diffuse reflectance images were acquired at 1Hz temporal resolution across 20 minutes for both the experimental cases. The rationale for imaging these two cases was th determine if any inherent

changes in diffuse reflectance occurred for these samples and determine the background baseline signal prior to introducing the reaction in study 2.

Data Analysis: Three regions of interest were selected – one on the target vessel and two background regions (away from the vessel). Two background regions were selected for comparison purposes – to determine if the selection of background region of interest (ROI) impacted the baseline signal. When the vessel was filled with DI water or methemoglobin without the reducing agent, it could be seen that the signal across time for each trendline was similar (see Fig. 4). With regards to the background ROI selected at two different locations in the imaged sample, it was inferred that selection of the background ROI did not impact the acquired diffuse reflectance signal. In particular for methemoglobin in the vessel (case 2), this implied the methemoglobin was not reacting under atmospheric conditions without the reducing agent. Now, in the presence of the reducing agent, a significant change in the oxygen saturation (calculated from diffuse reflectance measurements) is expected in the phantom (as described in Study 2).

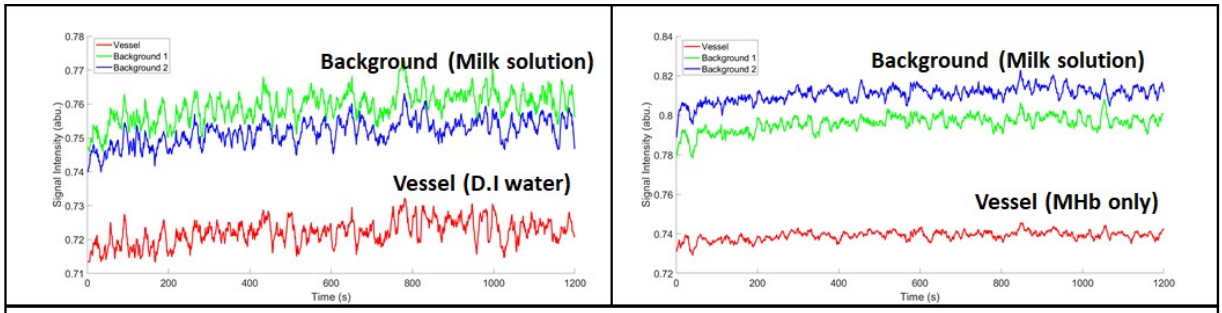

Figure 4. Phantom studies with scattering background. Diffuse reflectance signals across 20 minutes acquired from the phantom, where the vessel was filled with (a) D.I. water, and (b) methemoglobin without any reactions in either. There was no change in the baseline measurements and the signal from the vessel is lesser than that of the background, due to differences in the scattering and absorption between vessel and background, but there is no change observed with time.

Study 2: In this study, the background of the phantom was still the milk-based solution, and the vessel included MHb and the reducing agent. Liquid phantom mimicking blood in tissues contained ~20 mL of oxygen per 100 mL of blood and HbT between 60-225 g/L. These phantoms were using MHb (from bovine hemoglobin) solution in the vessel and diluted milk solution for the background. Changes in tissue oxygenation (or hemoglobin parameters) were produced by a controlled reduction of MHb, using sodium hydrosulfite ($Na_2S_2O_4$ + 2MHb → 2HbR + $2NaHO_3$). Pure oxygen (O_2 ≥ 99.5%) was introduced to form HbO in a closed, dynamic circulating system (measured by an oxygen sensor) (see Fig. 5). Our hand-held NIRS device (NIROS) was used to dynamically image during the entire reaction, along with discrete measurements using a commercial dissolved oxygen (DO) meter (every 30 seconds). With time, methemoglobin (MHb) solutions were reduced to HbR using sodium hydrosulfite (Na2S2O4) and converted to HbO. *Data Analysis*: Time-varying diffuse reflectance images acquired were used along with modified Beer-Lambert's law to determine the changes in oxygen saturation (StO_2) during the 60 min imaging study. Time-varying StO_2 changes recorded in response to the reaction between MHb and $Na_2S_2O_4$ using our NIRS-based device (and applying 2-λ MBLL model) showed >91.8% correlation to DO meter measurements. Thus, the NIROS device is validated and demonstrates the ability to measure oxygenation changes in a tissue-mimicking scattering medium. Current evidence indicates that NIROS is capable of measuring real-time hemoglobin-based oxygenation changes, and the device is validated via phantom studies.

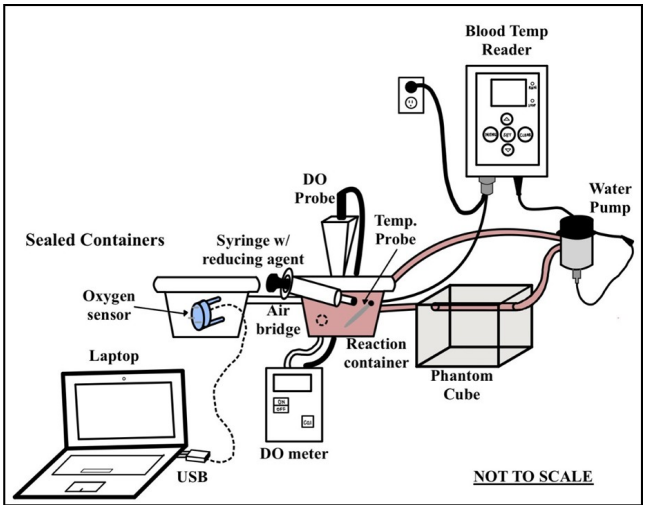

Fig 5. Phantom set-up to validate NIROS device vs. dissolved oxygen (DO) meter.

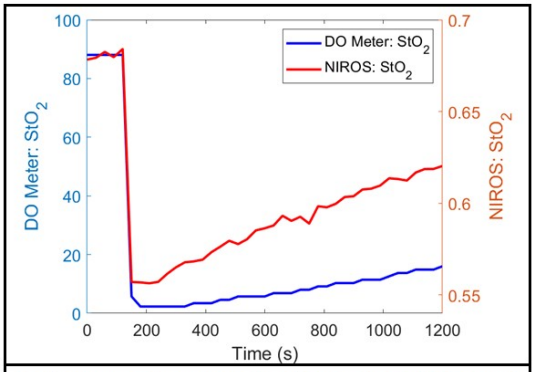

Fig 6. Changes in oxygen saturation in the first 20 min of the reaction between MHb and sodium hydrosulfite in the vessel, as observed by our NIROS device and a standard dissolved oxygen (DO) meter. The Pearson's correlation was > 91%.

AIM 2: Develop a quantifiable TO biomarker for assessing healing of DFUs across weeks of treatment.

Prior to studies on DFU cases, validation studies in-vivo on control subjects was carried out using NIROS and a commercial device to validate the ability of NIROS to obtain similar tissue oxygenation changes (as that of the commercial device).

Fig 7. : Near Infrared Optical Scanner (NIROS) operated using a laptop and stabilized using an articulating arm.

(i) In-vivo validation of NIROS against a commercial device [3,4, ongoing]:

In this study, NIROS' ability to acquire 2D spatial and temporal maps of tissue oxygenation at a high sampling rate (10Hz) has been developed. The ability to obtain spatial-temporal maps was via standard occlusion studies was performed, and the results validated using a commercial multispectral imaging device (capable of obtaining 2D spatial TO maps).

Instrumentation of NIROS for dynamic imaging: NIROS was modified to allow dynamic imaging at a high sampling rate (10Hz). NIROS utilizes multi-wavelength LEDs in the 650-900nm range to illuminate the tissue region of interest at 8mW of optical power per wavelength per LED (see Fig. 7). This study utilized 690nm and 830nm to acquire 2D dynamic diffuse reflectance signals (at each wavelength) up to 10Hz frequency. A custom MATLAB-based GUI was used to record these diffuse reflectance signals detected by NIR sensitive CMOS camera, which are in turn processed to obtain 2D tissue oxygenation maps in terms of effective oxy- (ΔHbO), deoxy- (ΔHbR), total hemoglobin (ΔHbT), and oxygen saturation (ΔStO_2) across time.

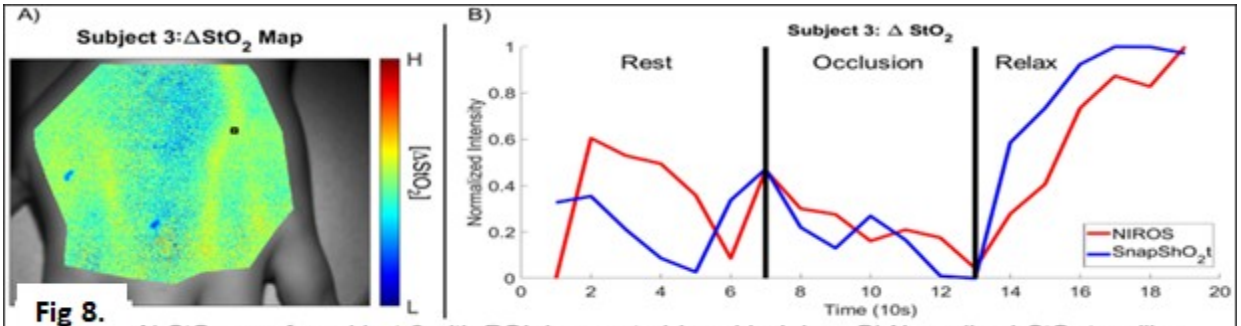

Fig 8. A) StO_2 map for subject 3 with ROI demarcated by a black box. B) Normalized StO_2 trendline from NIROS (red) and the commercial device (blue).

In-vivo studies: Healthy control subjects are recruited with IRB approval from FIU, with datasets from 3 subjects provided. All subjects were imaged on the hand (dorsal) using an upper arm occlusion paradigm. The paradigm utilized is 3 minutes long and consists of a 50 sec resting period, 10-sec occluding period, 60 sec of full occlusion, and 60 sec relaxation period. The occlusion pressure was set to 30 mm Hg over the subject's systolic pressure. These validation studies showed ~90% correlation in ΔStO_2 changes in response to occlusion when compared to a commercial device employing similar NIRS technology (SnapShO_2t, Kent) (see Fig. 8).

(ii) In-vivo imaging studies of DFUs across weeks of treatment using NIROS:

In-vivo imaging studies on DFUs were carried out using NIROS at the Univ of Miami Wound Care Center (Consortium-PI, Kirsner).

Subject Recruitment: 11 ulcerated subjects (10 DFU & 1 non-DFU) were recruited in this study. Of the 10 subjects, 5 subjects were imaged (1 Non-DFU and 4 DFU) for 4+ weeks or until the wound healed. 6 subjects were not completed due to the onset of the COVID-19 pandemic in 2020 (2 subjects) and due to subject transfer to other clinics (3 subjects). 3 subjects completely healed (1 non-DFU & 2 DFU) (see Table 1).

Subject	Wound Type	Imaged for 4+ weeks or healed?	Current Status
UM 001	Non-DFU	Yes	Healed
UM 002	DFU	No	Dismissed due to COVID-19 pandemic
UM 003	DFU	No	Dismissed due to COVID-19 pandemic
UM 004	DFU	No	Dismissed due to COVID-19 pandemic
UM 005	DFU	Yes	Completed 4+ weeks of imaging
UM 006	DFU	Yes	Healed
UM 007	DFU	Yes	Completed 4+ weeks of imaging
UM 008	DFU	Yes	Healed
UM 009	DFU	No	Transferred to new clinic
UM 010	DFU	No	Transferred to new clinic
UM 011	DFU	No	Transferred to new clinic

Table 1. Details of the recruited subjects at the UM Wound Care Center for wound imaging studies using NIROS.

Methodology: Diffusedly reflected NIR images were acquired thrice per wound at different angles across 4+ weeks of treatment. From the NIR images, hemoglobin-based oxygenation maps (in terms of Oxy-, Deoxy-, total hemoglobin, and oxygen saturation) were calculated. In addition to NIR images, color images of the wound were also acquired. From the oxygenation maps, three regions of interest were selected from the wound, peri-wound, and background tissue to calculate contrast values in terms of Wound-to-background, Wound-to-periwound, and Periwound-to-background to assess how tissue oxygenation changed across weeks of treatment.

Results and Discussion: Oxygen saturation maps across weeks of treatment were acquired and is shown for one case of a non-healing DFU and a healing DFU in Fig. 9 and 10, respectively. It is not obvious from these 2D pseudo-color plots if the differences in oxygen saturation between the wound, peri-wound and background depict when the wound is towards healing or non-healing. Hence relative contrast values were developed for Wound:Background, Wound:Peri-Wound, and Peri-Wound:Background and plotted against wound size (area) across weeks of treatment, as shown in Fig. 11 and 12 for non-healing and healing DFU cases, respectively. In the non-healing DFU case, as the wound size increased, the wound:background contrast and the wound-peri-wound contrast increased at both the chosen locations for quantitative analysis. In other words, the oxygen saturation was higher in the wound compared to the peri-wound and the background. There is no synchronous correlation between peri-wound:background contrast vs. wound size. However, it was interesting to observe that the peri-wound has lower oxygen saturation most of the weeks compared to the background region that is far away from the wound (as observed in both chosen regions in Fig 11, last column.

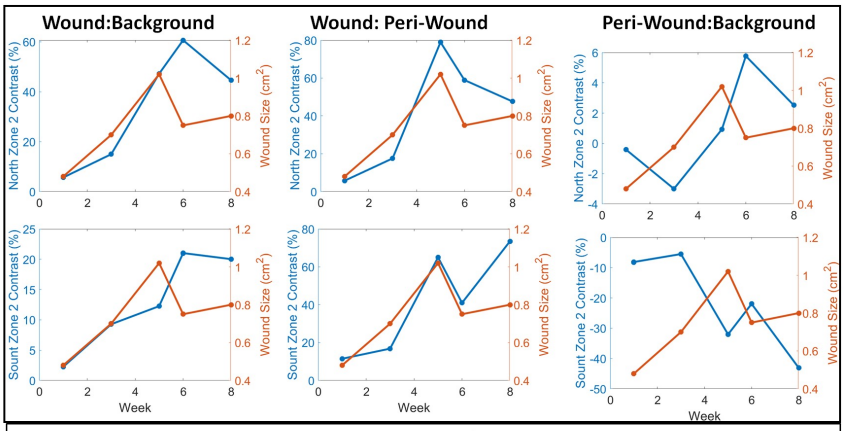

Fig 11. Relative contrast ratios in terms of wound:background, wound:peri-wound, and peri-wound:background of a **non-healing DFU** across weeks of treatment, in comparison to the wound area (as measured by the clinician). The top row was using background and peri-wound picked at the top of the wound, and the bottom row picked below the wound (i.e. two independent locations).

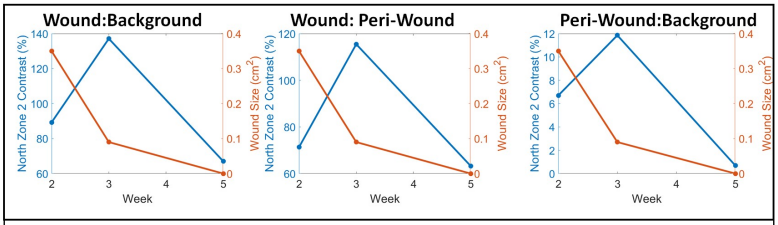

Fig 12. Relative contrast ratios in terms of wound:background, wound:peri-wound, and peri-wound:background of a **healing DFU** across weeks of treatment, in comparison to the wound area (as measured by the clinician).

In the healing DFU case, as the wound size is decreased, the wound:background, wound:peri-wound, and peri-wound:background contrast increase and drop with weeks of treatment. This trend is opposite to that observed in the non-healing wound (in Fig. 11). In the peri-wound:background contrast, it was interesting to observe that the contrast always remained positive and reached close to zero by week-5 (when the DFU healed), unlike a negative contrast in the non-healing DFU case (in Fig. 11). This demonstrates that higher oxygen saturation in the peri-wound compared to the background is an indicator that the wound would heal, compared to the case where the oxygen saturation immediately around the wound (i.e., peri-wound) is much smaller than the background, which indicates possible non-healing or yet to heal.

Conclusions: A hand-held near-infrared optical scanner (NIROS) was validated via phantom studies with >90% correlation in oxygen saturation changes as observed by a dissolved oxygen meter during a dynamic chemical reaction. Preliminary in-vivo validation studies on control subjects in response to occlusion demonstrated ~90% correlation in oxygen saturation changes in comparison to that observed using a commercial device. Studies on DFUs demonstrated that the oxygen saturation changes across weeks differed between healing and non-healing cases and that the oxygen saturation in the peri-wound compared to the background was a possible indicator of potential healing (negative when non-healing and positive when healing). Future work involves developing the NIROS imaging technology for extensive clinical imaging as well as for dynamic image analysis.

3. Publications/Presentations:

1. M. Sailaijiang, "*Validation of a Near-Infrared Optical Scanner to Measure Changes in Oxygenation: Phantom Studies,"* MS Project, Florida International University, April 2019.

2. M. Sailaijiang, K. Kaile, A. Godavarty *"Validation of a near-infrared optical scanner to measure changes in oxygenation: Phantom studies*," BME Graduate Research Day, FIU, Feb 2019 (Poster).

3. J. Barter, K. Leiva, E. Robledo, A. Godavarty, **"***Automation of Image Analysis for Real-Time Oxygenation Imaging of Wounds,"* BMES Annual Meeting Oct 16-19, 2019 (Poster Presentation).

4. K. Leiva, and A. Godavarty. "Variations in oxygenation flow patterns from breath-hold paradigm as a potential biomarker in differentiating normal to diseased tissues." Advanced Biomedical and Clinical Diagnostic and Surgical Guidance Systems XIX. Vol. 11631. International Society for Optics and Photonics, 2021. (ORAL) & Conference proceedings

5. K. Leiva, E. Robledo, D. Ortega, W. Wu, A. Godavarty, "In-Vivo validation of a Near-Infrared Optical Scanner (NIROS) via an occlusion paradigm," FIU BME Graduate Research Day, March 6, 2020 (POSTER)

6. K. Leiva, E. Robledo, D. Ortega, W. Wu, and A. Godavarty, "Dynamic Tissue Oxygenation Measurements from a Hand-Held Near-Infrared Optical Scanner (NIROS): In-vivo Validation Studies," in Biophotonics Congress: Biomedical Optics 2020 (Translational, Microscopy, OCT, OTS, BRAIN), OSA Technical Digest (Optical Society of America, 2020), paper TM3B.4. (ORAL) & Conference Proceedings

7. V. Roldan, K. Leiva, K. Kaile, M. Weigelt, A. Espinoza, R. Kirsner, A. Godavarty, "Data Analysis of Images Obtained with Two Near-Infrared Devices for Static Imaging and Dynamic Imaging with a Breath-Hold Paradigm in Patients with Diabetic Foot Ulcers," FIU BME Undergraduate Research Day, September 25, 2020 (POSTER)

8. V. Roldan, K. Leiva, K. Kaile, M. Weigelt, A. Espinoza, R. Kirsner, A. Godavarty, "Spatial-Temporal Maps of Oxygen Saturation in Foot Ulcers Using A Near-Infrared Optical Scanner," BMES 2020 Virtual Annual Meeting, October 14-17, 2020 (POSTER)

9. K. Leiva, K. Kaile, V. Roldan, M. Weigelt , A. Espinoza, R. Kirsner, W. Wu, A. Godavarty, "Spatio-Temporal Mapping of Oxygenation Changes in Foot Ulcers," Innovations in Wound Healing Conference (Virtual), Dec. 11-13, 2020 (POSTER)